

## Phase-slip dissipation and dimensionality above the irreversibility line in $\text{Bi}_2\text{Sr}_2\text{CaCu}_2\text{O}_{8+x}$

M. Giura, S. Sarti, E. Silva, R. Fastampa, and F. Murtas

*Dipartimento di Fisica, Università "La Sapienza," Piazzale Aldo Moro 2, 00185 Roma, Italy*

R. Marcon

*Dipartimento di Fisica "E. Amaldi," III Università di Roma, Roma, Italy*

H. Adrian and P. Wagner

*Institut für Festkörperphysik, Technische Hochschule Darmstadt, 64289 Darmstadt, Germany*

(Received 5 May 1994; revised manuscript received 8 July 1994)

The analysis of several sets of data for the resistivity in  $\text{Bi}_2\text{Sr}_2\text{CaCu}_2\text{O}_{8+x}$  films, measured as a function of the temperature, the magnetic field, and the field orientation, allows us to show that a phase-slip-dissipation model is able to accurately describe the experimental results when the fluxon thermal fluctuations are governed by a glasslike activation law  $A/[T - T_g(H)]$ , where  $T_g(H)$  is the irreversibility line. In this framework, we obtain the temperature and magnetic-field dependence of the quasi-activation-energy  $A$ . A qualitative explanation is given for the temperature and magnetic behavior in terms of a 3D-2D crossover due to the softening of the flux lines with increasing field.

### I. INTRODUCTION

Recently, there has been a good deal of discussion about the actual nature of the dissipation processes in high- $T_c$  superconductors (HTCS's) in the presence of a magnetic field. Various interpretations have been proposed to explain the mechanism by which the fluxon system gives rise to dissipation. The first explanation of the magnetic-resistive behavior was given in the traditional framework based on the conventional flux creep and flux flow. However, various inconsistencies have been found in the application of this model, the main one being the assumption that the Lorentz force causes the fluxon dissipation. As it is well known, no dependence of the dissipation on the relative angle between the current  $I$  and the magnetic field  $H$  has been observed in  $\text{Bi}_2\text{Sr}_2\text{CaCu}_2\text{O}_{8+x}$ ,<sup>1,2</sup> indicating the experimental lack for the Lorentz force in this superconductor family. Further, also in  $\text{YBa}_2\text{Cu}_3\text{O}_7$ , in which a Lorentz-force-like contribution has been found, the application of a creep model turns out to be cumbersome and needs questionable *ad hoc* hypotheses.<sup>3</sup> Thus, the experimental frame seems to indicate that a conventional flux motion framework is inadequate to give a coherent interpretation of the magnetic resistive measurements.

We have shown in the past that, by applying an alternative dissipation model, it is possible to give an overall interpretation of the resistive transition in the presence of a static magnetic field both in  $\text{YBa}_2\text{Cu}_3\text{O}_7$  and in  $\text{Bi}_2\text{Sr}_2\text{CaCu}_2\text{O}_{8+x}$ .<sup>4,5</sup> The model can be summarized by the following points:

(i) existence of a vortex solid phase, below a field-dependent temperature  $T_g(H)$ , in which the system of fluxons is practically motionless and the dissipation is not detectable.

(ii) the dissipation at temperatures greater than  $T_g(H)$  is due to thermal fluctuations of fluxons over a region of

inhomogeneities of the phase of the order parameter (phase slippage).

Within this model, the irreversibility line  $T_{\text{irr}}(H)$  present in the  $H$ - $T$  phase diagram of HTCS's is interpreted as the transition line  $T_g(H)$  between the solid glass phase and the fluid phase of the fluxons system. The main point of our model is that above  $T_g(H)$  the thermal fluctuations are governed by a glasslike activation law, that is the usual  $U/k_B T$  term has to be replaced by the expression  $A/[T - T_g(H)]$ , where  $A$  is a quasi-activation-energy.

In the present work, we focus our attention on the behavior of the physical quantities involved in the presented model for the measured dissipation in several  $\text{Bi}_2\text{Sr}_2\text{CaCu}_2\text{O}_{8+x}$  samples. From our data, we extract the temperature and magnetic dependence of the quasi-activation-energy  $A(H, T)$ . We find that the magnetic dependence of  $A(H, T)$  exhibits a nearly temperature-independent broad maximum around a few kilogauss. We show that above this characteristic field an angular scaling of the resistivity data occurs. We find also that the obtained irreversibility line presents a change of curvature in correspondence of the same field. All these results are obtained through the analysis of several sets of data for the resistivity, measured as a function of the temperature, the magnetic field, and the field orientation  $\vartheta$  with respect to the  $(a, b)$  planes. A consistent explanation of all the previously summarized features is given in the following, in terms of a three-dimensional-two-dimensional (3D-2D) crossover due to the softening of the flux lines in the  $c$  direction with increasing magnetic field.

### II. EXPERIMENT

#### A. Setup and samples

A set of resistivity measurements on  $\text{Bi}_2\text{Sr}_2\text{CaCu}_2\text{O}_{8+x}$  films grown with different techniques is presented. The

TABLE I. In the table are reported the critical temperatures  $T_c$  and the transition widths  $\Delta T_c$  for our samples.  $T_c$  is determined as the temperature corresponding to inflection point of the resistive transition curve and  $\Delta T_c$  as the temperature width corresponding to [90–10] % of the same curve.

Sample	$T_c$ (K)	$\Delta T_c$ (K)
I	82.3	7.38
IIa	83.5	4.45
IIb	86.5	5.25
III	88.9	14.0

samples I, IIa, and IIb, grown by liquid-phase epitaxy<sup>6</sup> (LPE), were about 1  $\mu\text{m}$  thick, 9 mm long, and 2 mm wide. The mosaic spread was less than 0.15°, according to x-ray diffraction. The sputtered film (sample III)<sup>7</sup> was about 0.3  $\mu\text{m}$  thick, 6 mm long, and 2 mm wide. In Table I, information about the transition temperatures and transition widths of these samples is also reported. The latter film exhibited a slow degradation with time and thermal cycles, showing a reduction of the zero-resistance temperature. This fact could be ascribed to the slow release of oxygen, as suggested by the fact that a successive reoxygenation restored the original features of the sample. Every set of measurements on this sample was taken in short-time intervals, and the stability of the sample for those intervals was checked by a daily repetition of the zero-field transition. Several sets of measurements were taken, with different degrees of degradation. As it will be seen, it is of interest to compare the overall properties of such a sample. The LPE films exhibited neither degradation nor change in the resistivity curves.

Voltage-drop measurements were taken by a lock-in version of the four-probe technique. The measuring frequency was 20 Hz. The probing current varied slightly from sample to sample, but it was always in the range 5–20  $\mu\text{A}$  (current densities are in the range 0.1–1  $\text{A}/\text{cm}^2$ ). The voltage sensitivity was about 5 nV. The temperature was measured by a Pt sensor, and was stabilized within 0.03 K during any fixed-temperature measurement.

The resistivity was then measured as a function of the temperature, the magnetic field, and the field orientation  $\vartheta$  with respect to the  $(a,b)$  planes. The measuring configuration was such that the probing current, which flowed in the  $a$ - $b$  plane, and the magnetic field were always mutually perpendicular. The angular accuracy was 0.1°. The maximum attainable field was 18 kG in the angular measurements, and 60 kG in the orthogonal-field measurements.

### B. Angular-dependent resistivity measurements and scaling properties

We have measured the voltage drop at fixed temperature  $T$ , as a function of the applied magnetic field  $H$ , for several angles  $\vartheta$ . In Fig. 1 we show the typical results for the voltage drop at fixed temperature, at various angles (sample I). As a consequence of the high anisotropy of the  $\text{Bi}_2\text{Sr}_2\text{CaCu}_2\text{O}_{8+x}$  compound, the resistivity drops

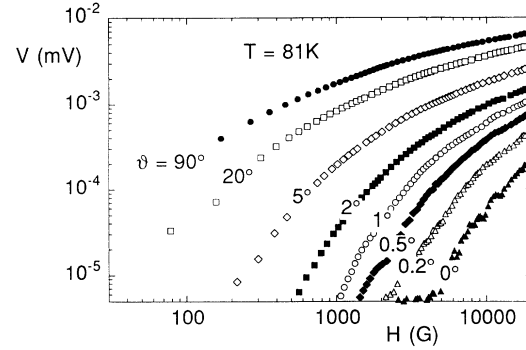


FIG. 1. Magnetoresistivity at fixed temperature for several angles between the field direction and the  $(a,b)$  plane:  $\vartheta=90^\circ$  (full circles),  $\vartheta=20^\circ$  (open squares),  $\vartheta=5^\circ$  (open diamonds),  $\vartheta=2^\circ$  (full squares),  $\vartheta=1^\circ$  (open circles),  $\vartheta=0.5^\circ$  (full diamonds),  $\vartheta=0.2^\circ$  (open triangles),  $\vartheta=0^\circ$  (full triangles). The observed dissipation is strongly depressed at angle near the parallel orientation, due to the large anisotropy of  $\text{Bi}_2\text{Sr}_2\text{CaCu}_2\text{O}_8$ .

dramatically approaching the parallel-field ( $\vartheta=0^\circ$ ) orientation. Due to the relatively low fields attainable in the variable-angle setup, any investigation of the dissipation for  $\vartheta \approx 0^\circ$  below  $T \approx 79$  K was not available. The angular measurements are thus confined to the temperature range close to  $T_c$ .

In these measurements, it is possible to identify an onset field for the dissipation, that comes out to be temperature—and angle—dependent. Detailed experimental investigations of these dependencies were given elsewhere.<sup>8–10</sup> We now focus the attention on the angular scaling properties of the entire resistivity curves  $\rho(H, \vartheta)$ .

The angular scaling procedure has been applied to several transport properties.<sup>11,12</sup> As a general rule, such procedure is successful when the  $H$  dependence and the  $\vartheta$  dependence of the transport property is of the type  $\rho(H, \vartheta) = \rho[H/f(\vartheta)]$ , where we have taken the resistivity as an example.

On theoretical grounds, it has been argued that such a dependence is obtained at least when no Lorentz force acts on the fluxon system.<sup>13</sup> This is exactly the situation in  $\text{Bi}_2\text{Sr}_2\text{CaCu}_2\text{O}_{8+x}$ , where both  $\rho_{ab}$  (Ref. 1) and  $\rho_c$  (Ref. 14) experiments demonstrate that there is no observable Lorentz force. The appropriate scaling function  $f(\vartheta)$  has been the subject of several papers. Anisotropic 3D,<sup>15</sup> coupled-layers,<sup>16</sup> and thin-film<sup>17</sup> expressions were employed in the scaling of various anisotropic properties.<sup>11,12</sup> In the present approach, we will leave  $f(\vartheta)$  as a scaling parameter, and we will compare successively the result to the appropriate function.

As first evidence, we have noted that the scaling of the entire resistivity curves is not possible: while for fields  $H > 2$  kG the data collapse well (Fig. 2), the lower-field tails deviate from a perfect scaling. This behavior is not unreasonable, and can be understood as follows: if a crossover from a 3D to a 2D behavior appears with increasing field, as it seems to be established by both angular measurements<sup>9,10</sup> and neutron diffraction,<sup>18</sup> the scal-

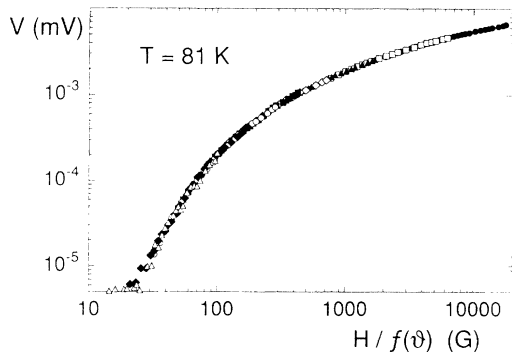


FIG. 2. Magnetoresistivity as a function of the reduced field  $H/f(\vartheta)$  for fields greater than 2 kG (see text). Same symbols as in Fig. 1. As can be seen, all the data collapse onto a single curve.

ing function changes with the field, so that a single-parameter scaling must not be expected. The result of the scaling procedure (data with  $H > 2$  kG) is shown in Fig. 2 for  $T = 81$  K, and it comes out to be extremely satisfactory. Consistently with the assumption of 2D behavior, we have found that the resulting scaling function has the shape given by the thin-film, quasi-2D Tinkham expression<sup>17</sup>

$$f_T(\vartheta) = \frac{1}{2\epsilon^{-2} \cos^2 \vartheta} \left[ \sqrt{\sin^2 \vartheta + 4\epsilon^{-2} \cos^2 \vartheta} - |\sin \vartheta| \right], \quad (1)$$

where the anisotropy ratio  $\epsilon$  is left as a fit parameter (Fig. 3). The fit is very good in the full  $\vartheta$  range, except very close to  $\vartheta = 0^\circ$ , where several transport measurements have shown the need for a much more complex theoretical treatment.<sup>19,20</sup>

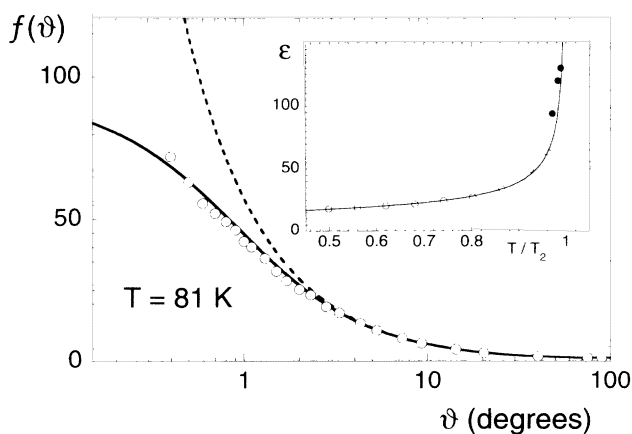


FIG. 3. Scaling function  $f(\vartheta)$ . In the same figure the prediction for the 2D case (continuous line) and the  $1/|\sin(\vartheta)|$  behavior are drawn. Apart from orientation very close to  $\vartheta = 0$  ( $\vartheta < 0.6^\circ$ ), the 2D prediction is fully verified. The  $|\sin \vartheta|$  scaling breaks down for relatively large angles. In the insert the anisotropy ratio data are shown. Full dots refer to the scaling of the resistivity for the sample IIb. Open circles refer to the scaling of  $J_c$  data shown in Ref. 12.  $T_2$ , defined as  $\epsilon^{-2}(T_2) = 0$ , is obtained through the linear fit of  $\epsilon^{-2}$  vs  $T$  (for details see Ref. 12).

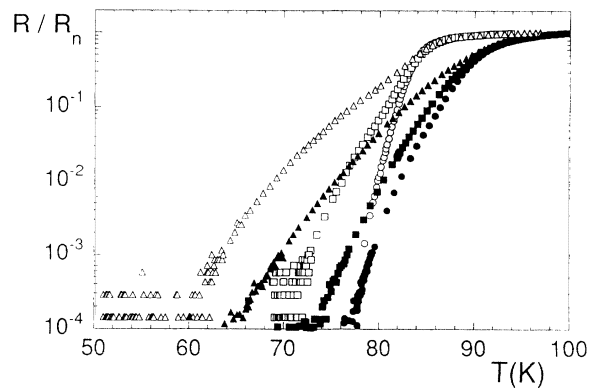


FIG. 4. Reduced resistivity  $R/R_n$  as a function of temperature for  $H = 0.1$  (circles), 0.5 (squares), and 2 kG (triangles), for sample II (open symbols) and sample III (full symbols).

The anisotropy ratio  $\epsilon$  is found to *increase* with increasing temperature: such a behavior is exactly what is expected by the quasi-2D model, in which  $\epsilon \sim (T - T_c)^{-1/2}$  (Ref. 17). A detailed discussion of the temperature-dependence of the anisotropy ratio has been given in Refs. 9, 12, 21, and 22.

In summary, our experimental results on the angular measurements of the resistivity are consistent with a 2D scaling for the data points with  $H > 2$  kG. The scaling breaks down for lower fields.

### C. Orthogonal-field resistivity measurements

The temperature range under investigation can be largely extended below 79 K by considering the orthogonal-field measurements, due to the much greater dissipation in the  $\vartheta = 90^\circ$  configuration. Such measurements were performed as a function of the temperature, at fixed magnetic fields [ $\rho_H(T)$ ], or as a function of the magnetic field, at fixed temperature [ $\rho_T(H)$ ]. In Fig. 4 we report typical data of the reduced resistivity defined as

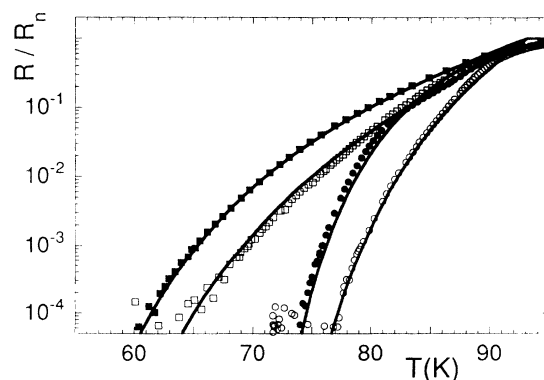


FIG. 5. Reduced resistivity  $R/R_n$  as a function of temperature for  $H = 0.1$  (circles) and 2 kG (squares) for sample III at different degradation stages (see text). Open symbols refer to first measured data, continuous lines are the fits obtained by Eqs. (2) and (3). To avoid crowding, only 10% of the experimental points is shown. Fits (continuous lines) are obtained by Eq. (2).

$\rho = R/R(100\text{ K})$  against the temperature at fixed magnetic fields for samples II and III, and in Fig. 5, the resistivity curves from a different set of measurements in sample III (as explained before) are shown.

The measurements shows a pronounced increase of the resistivity above some magnetic-field-dependent temperature. Below these thresholds the resistivity is negligible, and experimentally undetectable. It is an experimental result that although different samples present different shapes of the  $\rho_H(T)$  curves in the dissipative regime, the experimental onset temperatures for the dissipation are almost the same (Figs. 4 and 5) for the same field.

### III. DISSIPATION MODEL AND DISCUSSION

The absence of an experimentally measurable effect of the Lorentz force acting on the flux lines<sup>1</sup> suggests a non-conventional dissipation in the high- $T_c$  superconductors. In previous papers, we developed a model for dissipation which overcome those difficulties, linking a fluctuation-induced dissipation mechanism with glassy dynamics of the flux lines system. We briefly recall the main points of the model, referring the reader to Refs. 4 and 5 for a detailed discussion.

As a first hypothesis, we assume that the dissipation in the presence of a magnetic field arises from the phase slippage due to the flux-line motion over a region of inhomogeneities of the phase of the order parameter,<sup>23</sup> analogously to the flux motion over a network of Josephson junctions.<sup>24</sup> The origin of these inhomogeneities can be due to an unavoidable disorder in real samples or to an intrinsic spatial phase modulation in the  $a, b$  plane. It is to be noted that the "size" of such inhomogeneity regions should be compared to the coherence length: taking into account the smallness of the latter one can deduce that, within this model, also nearly atomic-scale inhomogeneities contribute to dissipation.

The second hypothesis is that the flux motion is an activated process of the glass type: the activation energy is finite only above the glass temperature  $T_g$  and, in the region above  $T_g$ , it follows a Vogel-Fulcher phenomenological behavior. Because of the conceptual difference between an ordinary activation energy and a glass expression, we will refer to the latter as "quasi-activation-energy."

The two hypotheses can be collected in the following expression for the reduced resistivity valid for low values of the current [ $J \ll J_c(0)$ ]:

$$\frac{R}{R_n} = \left[ I_0 \left[ \frac{\gamma(H, T)}{2} \right] \right]^{-2}, \quad (2)$$

where

$$\frac{\gamma}{2} = \frac{A(H, T)}{T - T_g(H)} \quad (3)$$

and  $I_0$  is the modified Bessel function of order zero.

While in the original Vogel-Fulcher expression,  $A$  does not depend on  $T$ , when such a conceptual frame is applied to the case of the superconducting system, a  $T$  dependence is expected, at least near  $T_c$ , due to the gra-

dual weakening of the superconductive parameters. This weakening naturally results in a lowering of the quasi-activation-energy for flux motion.

To proceed with the fit of the data, as a starting point for the determination of the parameters  $T_g$  and  $A$  we assume that

$$A(H, T) = A_1(H) A_2(T). \quad (4)$$

Performing the fits, we note that the parameter  $T_g(H)$  is not strongly dependent on the particular choice of the form of  $A_2(T)$ , if  $A_2$  is assumed to be a slowly varying function of  $T$  far from  $T_c$  (this assumption is consistent with the expected temperature dependence of  $A$ : far from  $T_c$ , the superconducting parameters are not expected to vary significantly with the temperature). In previous papers, we have shown that an expression such as

$$A_2(T) = \left[ 1 - \left[ \frac{T}{T_c} \right]^4 \right]^{1/2}, \quad (5)$$

is well suited both for  $\text{YBa}_2\text{Cu}_3\text{O}_7$  and  $\text{Bi}_2\text{Sr}_2\text{CaCu}_2\text{O}_{8+x}$ .<sup>4</sup> Using Eq. (4) in expression (2) for the resistivity, one is left with  $T_g(H)$  and  $A_1(H)$  as fit parameters. These parameters are easily obtained from the fits of the curves  $\rho_H(T)$  at fixed values of  $H$ . Typical fits are shown in Fig. 5. The consistency of the assumption (5) has been checked by considering the  $\rho_T(H)$  data, as explained in the Appendix.

We stress that the  $A_2(T)$  behavior is completely different from those predicted for the temperature dependence of the activation energy in the conventional theories of type-II superconductors. In these theories, the thermally activated flux motion is described by means of the activation term  $\exp\{U(B, J, T)/k_B T\}$ , where  $B$  is the magnetic induction and  $J$  is the current density in the hypothesis of linear relation between the current and the gradient  $\nabla B$ . The resulting pinning energy as a function of the temperature, obtained by fitting the data for the high- $T_c$  cuprates, shows an unusual maximum<sup>25</sup> and *ad hoc* hypotheses are needed to take into account this anomalous behavior.<sup>3</sup> The square-root behavior of Eq. (5), instead, is representative of the temperature dependence of the energy coupling in a Josephson-junction strong coupling,<sup>26</sup> consistently with the dissipation mechanism assumed in our model.

In Fig. 6 we report the behavior of the magnetic-field dependence of the  $A_1(H)$  at fixed temperature for all the samples under study. The magnetic-field dependence  $A_1(H)$  of the quasi-activation-energy sharply increases at low values of the magnetic field and then slowly decreases in the high magnetic field range (Fig. 6), resulting in a broad maximum in the kG range.

In Fig. 7 we report the behavior of  $T_g$  as a function of  $H$  (we reported in previous papers<sup>4,5</sup> that  $T_g$  as achieved in our model reproduces quite well the commonly obtained irreversibility line measured by means of several techniques).

While it is evident that the model proposed accurately describes the magnetic dependence of the resistivity, and the temperature dependence  $A_2(T)$  can be understood

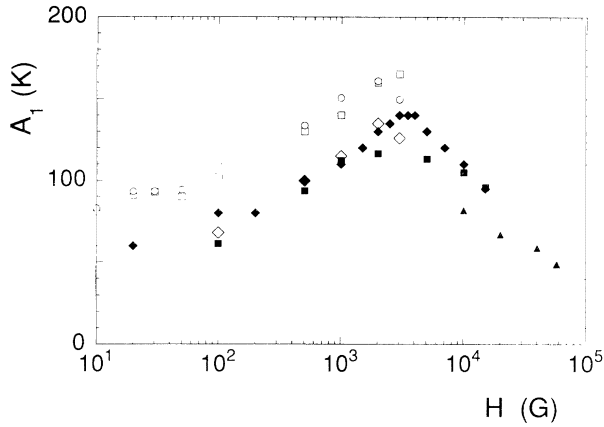


FIG. 6. Magnetic-field dependence  $A_1(H)$  of the quasi-activation-energy for all the measured samples: sample I (full diamonds), sample IIa (full squares), sample IIb (full triangles), and sample III (empty circles, squares and diamonds) at three different degradation stages.

within the Josephson-junction nature of the dissipation in this model, an explanation of the general features of the magnetic behavior of  $A_1(H)$  and  $T_g(H)$  is needed.

First, as it can be seen in Fig. 7,  $T_g(H)$ , when plotted in the usual log-lin scale, shows an inversion of curvature in the kG region. This change of curvature has been interpreted<sup>27</sup> as a magnetically induced 3D-2D crossover, due to the progressive weakening, as the field is increased, of the flux rigidity.<sup>28,29</sup>

Regarding the magnetic behavior of the quasi-activation-energy, because of the connection of the dissipation mechanism here described with the motion of the flux lines in the fluid state (as opposed to the solid state below  $T_g$ ), one is led to some analogy with the well-known theories of pinning. In analogy with the behavior of the pinning force, one could try to explain the qualitative features of  $A_1(H)$  with the traditional model of Kramer.<sup>30</sup> It refers to the elastic energy stored in the flux-line lattice (FLL) when it is in static interaction with the

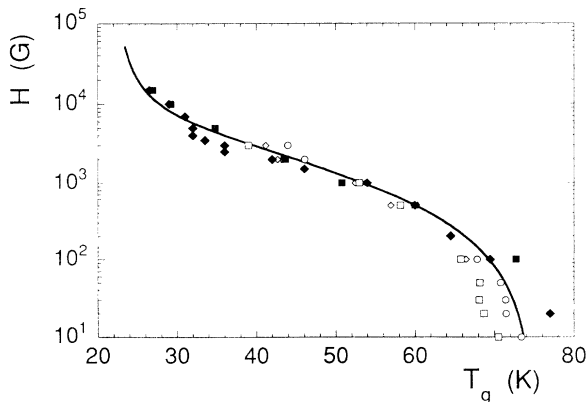


FIG. 7. Irreversibility line for all measured samples. Symbols are the same as in Fig. 6. An inversion of curvature is evident in the kG region. Continuous line is a guide for eye.

pin system. At low magnetic field the pinning increases when the FLL is subjected to two types of pins, a large number of individual point pins and a small number of strong line pins. Increasing the magnetic field and then the Lorentz force, the elastic deformation becomes larger, the nearest flux lines to a strongly pinned one will move, sampling other pin arrangements. The number of the point pins along this flux line increases and the probability that the flux line itself will be strongly pinned raises. As a result, the number of the flux lines strongly pinned increases with the magnetic field. At high magnetic field, the line-pinning forces produce plastic deformation of the FLL when the shear stresses exceed the shear strength. The latter is proportional to the FLL shear modulus  $C_{66}$  which is a decreasing function of  $H$ , as pinning force indeed will result. It is possible to show that the pinning force is a function of the magnetic field only through the reduced field  $h = H/H_{c2}(T)$  (Ref. 30) and, as a consequence, the shape of the field dependence of the activation energy should depend on the temperature. The qualitative feature emerging from the present work, consistent in a temperature-independent maximum for  $A_1(H)$ , cannot be reconciled with the results of this model. Furthermore, the Kramer's model is founded on the balance between the Lorentz force acting on the flux lines and the pinning forces, so that a deeper objection to this framework lies in the experimental lack of the Lorentz force in  $\text{Bi}_2\text{Sr}_2\text{CaCu}_2\text{O}_{8+x}$ .

The main experimental finding of the appearance of a maximum in  $A_1(H)$  can be explained by some sort of matching between the flux lattice and the pinning site distribution: increasing the magnetic field, the distance between the fluxons decreases to the dominant spacing between pins,  $a_0$ , and at the corresponding magnetic field the pinning efficacy is maximum. In a conventional frame<sup>31</sup> the flux-lattice parameter is supposed to be independent from the temperature, and the matching condition at the field  $H = H_{\text{max}} \approx 3$  kG gives for the spacing  $a_0$  the value  $a_0 \approx (\Phi_0/B_{\text{max}})^{1/2} \approx 1000$  Å. This model, which could explain the independence of the  $H_{\text{max}}$  from the temperature, gives a too large spacing between the pins.

Keeping the validity of the general concept of matching between the fluxons system and some kind of pinning, a qualitative description can be given as follows: assuming the existence of a large number of point pins, the increasing of the pinning effectiveness at low magnetic field can be related to the softening of the flux line, which allows a better arrangement of the line itself on a larger number of the point pins. The origin of the softening in this case is assumed to be due to the reduction of the coupling between  $\text{CuO}_2$  planes induced by the magnetic field. By increasing the magnetic field, the in-plane fluctuations of the vortex becomes larger and larger, so that the correlation of the flux line over different  $\text{CuO}_2$  layers is almost lost. As a consequence, the vortex system crosses over from a 3D to a 2D behavior. This view is consistent with both experimental and theoretical results on highly layered superconductors, and the crossover field is about 2–3 kG.<sup>10,27,28</sup> This value is in accordance with the field

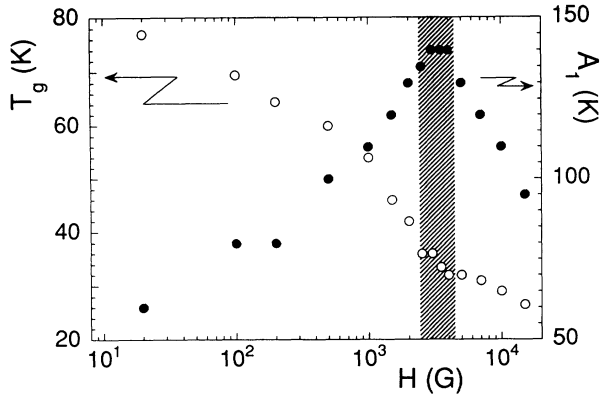


FIG. 8. Irreversibility line (open circles, left scale) and quasi-activation-energy (full circles, right scale) for sample I. The maximum of  $A_1(H)$  is in the same field range (dashed zone) as the change in curvature of  $T_g(H)$ .

at which the measured  $T_g(H)$  changes its curvature (Fig. 8). More, the angular measurements of  $\rho_T(H)$  scale in the whole angular range only if the data above  $H = 2$  kG are considered, and the resulting scaling function is well fitted by the one predicted for a 2D superconductor (see Fig. 2).

At sufficiently high fluxon density the interaction between the flux lines (which are now described in terms of “pancake” fluxoids,<sup>32</sup> because of the crossover to a 2D system) overcomes the interaction with the pinning centers, so that the magnetic activation energy is not expected to depend on the details of the pinning. The simultaneous effect of such a crossover in the flux matter on both  $A_1(H)$  and  $T_g(H)$  can be observed in Fig. 8. It is immediately apparent that the maximum of  $A_1(H)$  appears in the same field region where  $T_g(H)$  changes curvature.

#### IV. CONCLUSIONS

In this paper we have presented a large set of resistivity measurements, taken as a function of temperature, the magnetic field, and the field orientation. All the measurements were successfully fitted by our previous model for the dissipation, based on the fluctuations of the vortex liquid over regions of inhomogeneities of the order parameter. The angular measurements were found to scale, according to the 2D angular function, for fields greater than 2 kG. The field dependence of the quasi-activation-energy has been qualitatively understood in terms of the interaction of the fluxon system with the pins ensemble, due to the flux-line softening. The softening is ascribed to intrinsic properties such as the 3D-2D crossover. Such a crossover, being induced by the field, has a very weak dependence on the temperature, or even no dependence at all, resulting in a  $T$ -independent position of the maximum of  $A_1(H)$ . We note that the field corresponding to the maximum in  $A_1(H)$  lies in the range where the

crossover field is expected to be, consistent with the explanation proposed.

#### APPENDIX

It is possible to check the consistency of the assumption of separability of the quasi-activation-energy, Eq. (4), and of the form of the temperature dependence of  $A$ , Eq. (5), by using also the field-sweeps data,  $\rho_T(H)$ . The consistency test proceeds as follows: from the  $\rho_T(H)$  data it is possible to directly obtain  $\gamma(H; T)$ , Eq. (3), as a function of the field, by inversion of Eq. (2). Because the field sweeps are taken for several temperatures, one has  $\gamma$  as a function of the field for the same temperatures. Now, by using the  $T_g(H)$  values as obtained from the  $\rho_H(T)$  data (see Sec. III), the  $A_1(H)$ 's at different temperatures can be extracted [this procedure can be employed because  $T_g(H)$  does not depend much on the explicit expression for the temperature dependence  $A_2(T)$  of the quasi-activation-energy]. Some of the resulting  $A_1(H)$ 's at different values of  $T$  are plotted in Fig. 9. The curves can be made to coincide with each other by a multiplying factor, indicating that the separability assumption works: the multiplying factor constitutes the  $T$  dependence of  $A$ , that is  $A_2(T)$ .

Accordingly to the magnetic dependence obtained in the paper, the  $A(H; T)$ 's show a maximum in correspondence of a field intensity of a few kilogauss. Taking the height of the maximum as representative for every curve, the plot of these points as a function of the temperature gives the experimental  $T$  dependence,  $A_2(T)$ . In the inset of Fig. 9 these data are compared with the  $[1 - (T/T_c)^4]^{1/2}$  behavior, Eq. (5). Good agreement is found. Note that the heights have been normalized to

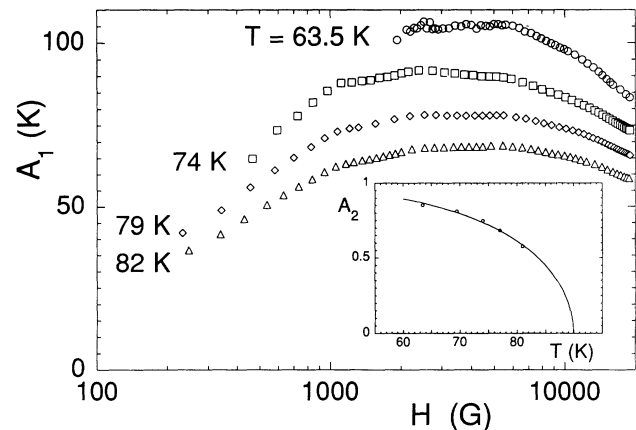


FIG. 9. Magnetic-field dependence  $A_1(H)$  of the quasi-activation-energy obtained directly by inversion of Eq. (2) (see text) for sample II. The inversion procedure is possible only if some signal is detected, so that the lower the temperature, the higher the first allowable value of field for which  $A_1(H)$  is available. The position of the maximum is nearly temperature independent. In the inset, the normalized height of the maximum as a function of  $T$  (empty symbols) and the predicted behavior  $[1 - (T/T_c)^4]^{1/2}$  (continuous line) are shown.

the  $T=0$  value (extrapolated), so as to have a dimensionless  $A_2(T)$  ranging from 0 to 1.

Collecting up the results of the consistency test, we are allowed to say that all the experimental data can be fitted

by the model summarized in Eqs. (2) and (3), and that the model is consistent with the assumption of separability, Eq. (4), and the temperature dependence of the quasi-activation-energy,  $A_2(T)$ , Eq. (5).

- 
- <sup>1</sup>Y. Iye, S. Nakamura, and T. Tamegai, *Physica C* **159**, 433 (1989); T. Fukami, T. Kamura, T. Yamamoto, and S. Mase, *ibid.* **160**, 391 (1989).
- <sup>2</sup>S. Labdi, H. Raffy, O. Laborde, and P. Monceau, *Physica C* **197**, 274 (1992).
- <sup>3</sup>C. W. Hagen and R. Griessen, *Phys. Rev. Lett.* **62**, 2857 (1988).
- <sup>4</sup>M. Giura, R. Marcon, E. Silva, and R. Fastampa, *Phys. Rev. B* **46**, 5753 (1992).
- <sup>5</sup>R. Fastampa, M. Giura, R. Marcon, S. Sarti, and E. Silva, *Supercond. Sci. Technol.* **6**, 53 (1993).
- <sup>6</sup>G. Balestrino, V. Foglietti, M. Marinelli, E. Milani, A. Paoletti, and P. Paroli, *Appl. Phys. Lett.* **57**, 2359 (1990).
- <sup>7</sup>P. Wagner, H. Adrian, and C. Tomé-Rosa, *Physica C* **195**, 258 (1992).
- <sup>8</sup>R. Fastampa, M. Giura, R. Marcon, and E. Silva, *Phys. Rev. Lett.* **67**, 1995 (1991); R. Marcon, E. Silva, R. Fastampa, and M. Giura, *Phys. Rev. B* **46**, 3612 (1992).
- <sup>9</sup>S. Sarti, E. Silva, R. Fastampa, M. Giura, and R. Marcon, *Phys. Rev. B* **49**, 556 (1994).
- <sup>10</sup>E. Silva, R. Marcon, R. Fastampa, M. Giura, and S. Sarti, *Physica C* **214**, 115 (1993).
- <sup>11</sup>H. Raffy, S. Labdi, O. Laborde, and P. Monceau, *Phys. Rev. Lett.* **66**, 2515 (1991).
- <sup>12</sup>R. Fastampa, S. Sarti, E. Silva, and E. Milani, *Phys. Rev. B* **49**, 15 959 (1994).
- <sup>13</sup>Z. Hao and J. R. Clem, *Phys. Rev. B* **47**, 5915 (1993).
- <sup>14</sup>M. Brinkmann, H. Somnitz, H. Bach, and K. Westerholt, *Physica C* **217**, 418 (1993).
- <sup>15</sup>A. A. Abrikosov, *Fundamentals of the Theory of Metals* (North-Holland, Amsterdam, 1988).
- <sup>16</sup>W. E. Lawrence and S. Doniach, *Proceedings of the 12th International Conference on Low Temperature Physics, Kyoto, Japan, 1970*, edited by E. Kanda (Kiegaku, Tokyo, 1971), pp. 361–362.
- <sup>17</sup>M. Tinkham, *Phys. Rev.* **129**, 2413 (1963).
- <sup>18</sup>R. Cubitt, E. M. Forgan, G. Yang, S. L. Lee, D. McK. Paul, H. A. Mook, M. Yethiraj, P. H. Kes, T. W. Li, A. A. Menovsky, Z. Tarnawski, and K. Mortensen, *Nature (London)* **365**, 407 (1993).
- <sup>19</sup>Y. Iye, T. Tamegai, and S. Nakamura, *Physica C* **174**, 227 (1991).
- <sup>20</sup>R. Fastampa, M. Giura, R. Marcon, and E. Silva, *Europhys. Lett.* **18**, 75 (1992).
- <sup>21</sup>R. A. Klemm, A. Luther, and M. R. Beasley, *Phys. Rev. B* **12**, 877 (1975).
- <sup>22</sup>T. Schneider and A. Schmidt, *Phys. Rev. B* **47**, 5915 (1993).
- <sup>23</sup>M. Tinkham, *Phys. Rev. Lett.* **61**, 1658 (1988).
- <sup>24</sup>V. Ambegaokar and B. I. Halperin, *Phys. Rev. Lett.* **25**, 1364 (1969).
- <sup>25</sup>D. O. Welch, *IEEE Trans. Magn.* **27**, 1133 (1991).
- <sup>26</sup>See, for example, I. O. Kulik and I. K. Yanson, *The Josephson Effect in Superconductive Tunneling Structures* (Wiener, Jerusalem, 1972), p. 112.
- <sup>27</sup>A. Schilling, R. Jin, J. D. Guo, and H. R. Ott, *Phys. Rev. Lett.* **71**, 1899 (1993).
- <sup>28</sup>L. I. Glazman and A. E. Koshelev, *Phys. Rev. B* **43**, 2835 (1991).
- <sup>29</sup>G. Deutscher and A. Kapitulnik, *Physica A* **168**, 338 (1990); S. Ryu, S. Doniach, G. Deutscher, and A. Kapitulnik, *Phys. Rev. Lett.* **68**, 710 (1992).
- <sup>30</sup>E. J. Kramer, *J. Appl. Phys.* **44**, 1360 (1973).
- <sup>31</sup>C. C. Kock and R. W. Carpenter, *Philos. Mag.* **25**, 303 (1972).
- <sup>32</sup>J. R. Clem, *Phys. Rev. B* **43**, 7837 (1991).